# DFT Study on the Mechanism and Regioselectivity of Gold(I)-Catalyzed Synthesis of Highly Substituted Furans Based on 1-(1-Alkynyl)cyclopropyl Ketones with Nucleophiles

Ran Fang,[†] Cheng-Yong Su,[†] Cunyuan Zhao,*[,†] and David Lee Phillips[‡]

*MOE Laboratory of Bioinorganic and Synthetic Chemistry, School of Chemistry and Chemical Engineering, Sun Yat-Sen University, Guangzhou 510275, People's Republic of China, and Department of Chemistry, The University of Hong Kong, Pokfulam Road, Hong Kong, People's Republic of China*

*Received August 3, 2008*

The mechanism and regioselectivity of gold(I)-catalyzed synthesis of highly substituted furans based on 1-(1-alkynyl)cyclopropyl ketones with nucleophiles have been investigated using density functional theory calculations done at the BH and HLYP/6-31G(d, p) (SDD for Au) level of theory. Solvent effects on these reactions have been explored by calculations that included a polarizable continuum model (PCM) for the solvent (dichloromethane). Our calculations suggest that the first step of the cycle is the cyclization of the carbonyl oxygen onto the triple bond to form a new and stable five-membered resonance structure of an oxonium ion and a carbocation intermediate. Furthermore, the seven-membered carbocation intermediate proposed by Zhang and Schmalz was found and characterized as a transition structure on the potential energy surface. The attack of the carbonyl oxygen to the gold-coordinated alkynes results in the formation of a resonance structure intermediate, which upon subsequent trapping with alcohols followed by migration of a hydrogen atom results in the formation of the final products and regeneration of the catalyst. The key reaction step is the attack of the oxygen atom of the $CH_3OH$ on the C−C $\sigma$ bond of the cyclopropane moiety to yield new organogold intermediates through formation of a C−O bond and cleavage of a C−C bond. The cleavage of the C−C bond is strongly favored kinetically in the case of the $C^1-C^2$ bond and required only 19.8 kcal/mol of energy, while the activation energy for cleavage of the $C^1-C^3$ bond was found to be 31.8 kcal/mol and indicates that the ring-opening cycloisomerization for cyclopropyl ketones has high regioselectivity. Our computational results are consistent with the experimental observations of Zhang and Schmalz for the gold(I)-catalyzed synthesis of highly substituted furans based on 1-(1-alkynyl)cyclopropyl ketones with nucleophiles.

## 1. Introduction

Highly substituted furans are an important group of heteroaromatic compounds that have been found in many natural products and substances that have useful industrial applications.[1] Highly substituted furans are also often used as synthetic intermediates in the preparation of acyclic, carbocyclic, and heterocyclic compounds.[2] Therefore, there has been much effort aimed at the development of synthetic methodology for the efficient preparation of substituted furans. One of these methodologies is based on cycloisomerization of (*Z*)-2-en-4-yn-1-ols,[3] and the Cu(II)-catalyzed large-scale preparation of 2,3-dimethylfuran starting from (*Z*)-3-methylpent-2-en-4-yn-1-ol provides an example of this.[4] A Ru-catalyzed synthesis of furans by selective cyclization of (*Z*)-enynols using $Ru(PPh_3)(p\text{-cymene})Cl_2$ as a catalyst precursor was reported by Dixneuf and co-workers,[5] and Liu and co-workers used gold as a catalyst for the cyclization of (*Z*)-enynols.[6] The cyclizations of allenyl ketones[7] and 3-alkyn-1-ones[8] using of Rh, Ag, and Pd as the catalyst precursor have also been detailed. $AuCl_3$-[9] and CuBr[10]-catalyzed cyclizations of 2-(1-alkynyl)-2-alken-1-ones to pro-

* Corresponding author. E-mail: ceszhcy@mail.sysu.edu.cn. Fax: 86-20-8411-0523. Phone: 86-20-8411-0523.

[†] Sun Yat-Sen University.

[‡] The University of Hong Kong.

(1) (a) Hou, X. L.; Cheung, H. Y.; Hon, T. Y.; Kwan, P. L.; Lo, T. H.; Tong, S. Y. T.; Wong, H. N. C. *Tetrahedron* **1998**, *54*, 1955. (b) Hou, X. L.; Yang, Z. Wong, H. N. C. In *Progress in Heterocyclic Chemistry*; Gribble, G. W., Gilchrist, T. L., Eds.; Pergamon: Oxford, 2002; Vol. 14, p 139. (c) Kirsch, S. F. *Org. Biomol. Chem.* **2006**, *4*, 2076. (d) Brown, R. C. D. *Angew. Chem., Int. Ed.* **2005**, *44*, 850.

(2) (a) Paquette, L. A.; Astles, P. C. *J. Org. Chem.* **1993**, *58*, 165. (b) Jacobi, P. A.; Touchette, K. M.; Selnick, H. G. *J. Org. Chem.* **1992**, *57*, 6305. (c) Paquette, L. A.; Doherty, A. M.; Rayner, C. M. *J. Am. Chem. Soc.* **1992**, *114*, 3910. (d) Martin, S. F.; Zinke, P. W. *J. Org. Chem.* **1991**, *56*, 6600. (e) Tanis, S. P.; Robinson, E. D.; McMills, M. C.; Watt, W. *J. Am. Chem. Soc.* **1992**, *114*, 8349.

(3) Gabriele, B.; Salerno, G.; Lauria, E. *J. Org. Chem.* **1999**, *64*, 7687, and references therein.

(4) Végh, D.; Zalupsky, P.; Kováč, J. *Synth. Commun.* **1990**, *20*, 1113.

(5) (a) Seiller, B.; Bruneau, C.; Dixneuf, P. H. *J. Chem. Soc., Chem. Commun.* **1994**, 493. (b) Kücükbay, H.; Cetinkaya, B.; Guesmi, S.; Dixneuf, P. H. *Organometallics* **1996**, *15*, 2434. (c) Seiller, B.; Bruneau, C.; Dixneuf, P. H. *Tetrahedron* **1995**, *51*, 13089.

(6) Liu, Y. H.; Song, F. J.; Song, Z. Q.; Liu, M. N.; Yan, B. *Org. Lett.* **2005**, *7*, 5408.

(7) (a) Hashmi, A. S. K. *Angew. Chem., Int. Ed.* **1995**, *34*, 1581. (b) Hashmi, A. S. K.; Ruppert, T. L.; Knofel, T.; Bats, J. W. *J. Org. Chem.* **1997**, *62*, 7295. (c) Hashmi, A. S. K.; L. Schwarz, L.; Choi, J. H.; Frost, T. M. *Angew. Chem., Int. Ed.* **2000**, *39*, 2285. (d) Ma, S.; Li, L. *Org. Lett.* **2002**, *4*, 941. (e) Ma, S.; Yu, Z. *Angew. Chem., Int. Ed.* **2002**, *41*, 1775. (f) Ma, S.; Zhang, J.; Lu, L. *Chem.−Eur. J.* **2003**, *9*, 2447. (g) Suhre, M. H.; Reif, M.; Kirsch, S. F. *Org. Lett.* **2005**, *7*, 3925.

(8) (a) Fukuda, Y.; Shiragami, H.; Utimoto, K.; Nozaki, H. *J. Org. Chem.* **1991**, *56*, 5816. (b) KelJin, A. V.; Gevorgyan, V. *J. Org. Chem.* **2002**, *67*, 95. (c) Sromek, A. W.; KelJin, A. V.; Gevorgyan, V. *Angew. Chem., Int. Ed.* **2004**, *43*, 2280.

(9) Yao, T. L.; Zhang, X. X.; Larock, R. C. *J. Am. Chem. Soc.* **2004**, *126*, 11164.

(10) Nitin, T.; Patil, Wu, H.; Yamamoto, Y. *J. Org. Chem.* **2005**, *70*, 4531.

10.1021/om800751u CCC: $40.75 
Publication on Web 01/07/2009

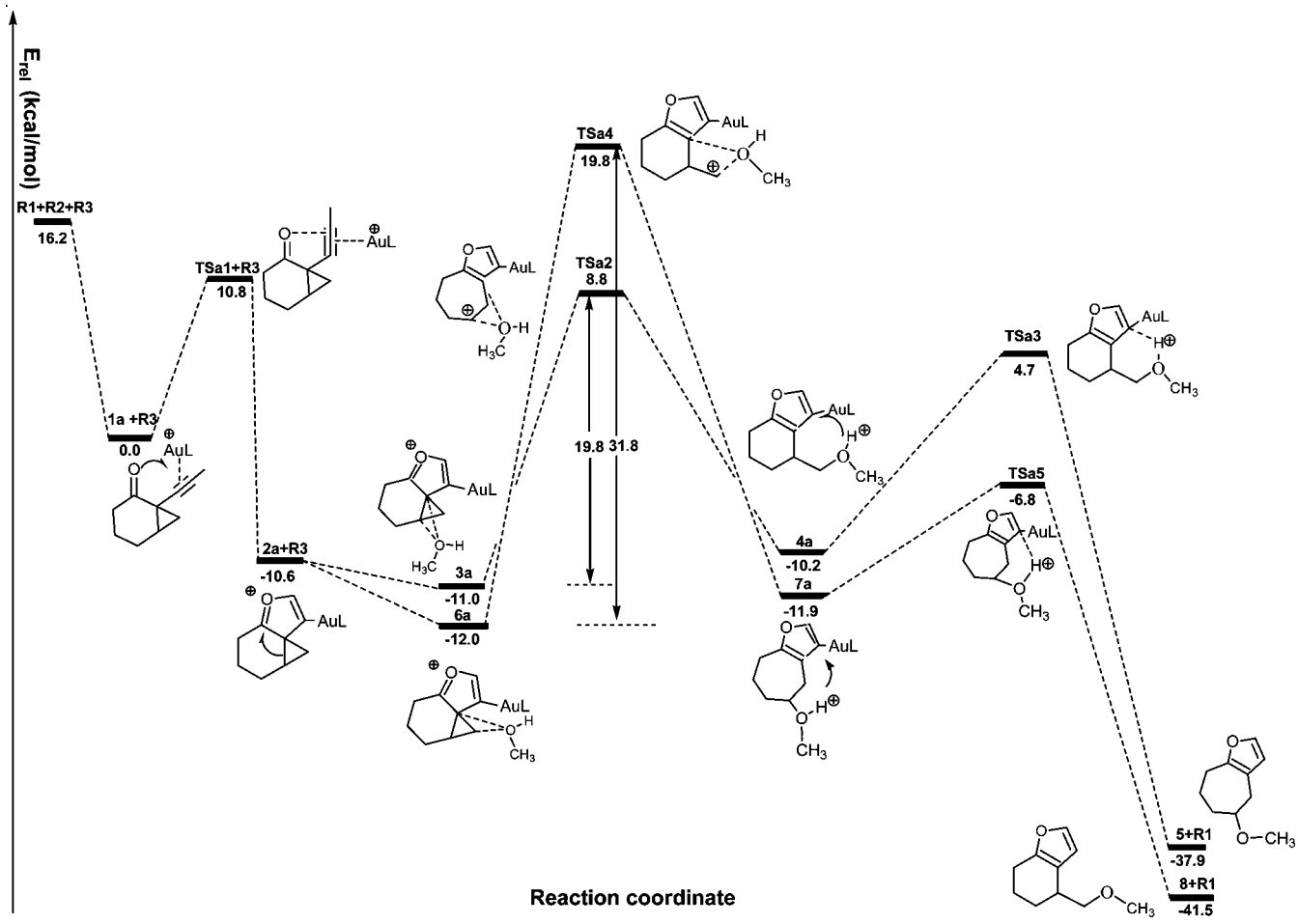


**Figure 1.** Energy profiles for path **a**; the relative energies are given in kcal/mol.

duce substituted furans have been reported, and the mechanisms of these reactions were proposed to take place via the formation of an oxonium ion that then reacts with nucleophiles to produce the corresponding products. The cycloisomerization of alkylidene cyclopropyl ketones[11] or cyclopropenyl ketones[12] can form furans through (regioselective) cleavage of the three-membered ring and subsequent cyclization. Gold homogeneous catalysis has been of increasing interest due to its many applications in organic synthesis.[13] Recently, gold(I)-catalyzed reactions were found to give efficient access to highly substituted furans under mild conditions by Zhang and Schmalz,[14] and two plausible mechanisms have been proposed for this novel gold(I)-catalyzed transformation (see Scheme 1). It is interesting to note that no reaction was observed when $Et_3SiH$ was employed as a potential hydride source in place of a nucleophile, and this appears to contradict a mechanism involving a carbocation intermediate.[14]

To our knowledge, there are no detailed theoretical studies available in the literature for the novel gold(I)-catalyzed transformation reported by Zhang and Schmalz.[14] Here, we present a detailed density functional theory (DFT) computational investigation of the mechanism and regioselectivity of the gold(I)-catalyzed synthesis of highly substituted furans. On the basis of the experimental evidence reported by Zhang and Schmalz,[14] it is possible to propose an even more detailed mechanism, as shown in Scheme 2. The structures of the possible intermediates involved in the various reaction pathways are based on those suggested in the literature. The present DFT study located the transition states for the reactions of interest, and we performed a vibrational analysis at these stationary points. From the results presented here, we hope to learn more

**Scheme 1. Two Plausible Mechanisms Were Envisioned for This Novel Gold(I)-Catalyzed Transformation**

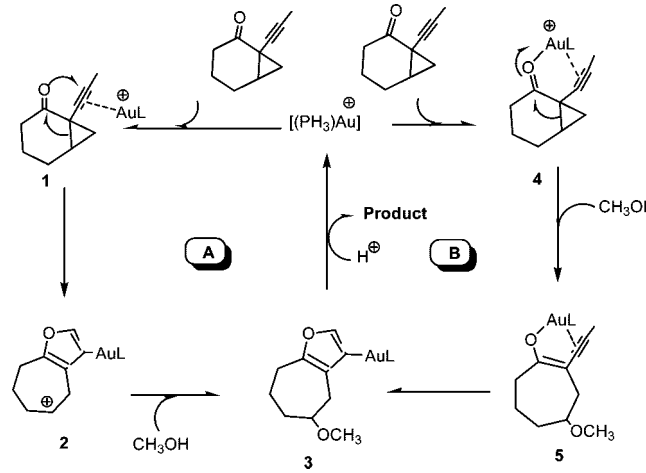


(11) (a) Ma, S.; Zhang, J. *Angew. Chem., Int. Ed.* **2003**, *42*, 184. (b) Ma, S.; Lu, L.; Zhang, J. *J. Am. Chem. Soc.* **2004**, *126*, 9645.

(12) (a) Padwa, A.; Kassir, J. M.; Xu, S. L. *J. Org. Chem.* **1991**, *56*, 6971. (b) Ma, S.; Zhang, J. *J. Am. Chem. Soc.* **2003**, *125*, 12386.

(13) (a) Gorin, D. J.; Toste, F. D. *Nature* **2007**, *446*, 395. (b) Stephen, A.; Hashmi, K. *Angew. Chem., Int. Ed.* **2008**, *47*, 6754. (c) Faza, O. N.; López, C. S.; Álvarez, R.; de Lera, R. *J. Am. Chem. Soc.* **2006**, *128*, 2434. (d) Nieto-Oberhuber, C.; Munoz, M. P.; Bunuel, E.; Nevado, C.; Cárdenas, D. J.; Echavarren, A. M. *Angew. Chem., Int. Ed.* **2004**, *43*, 2402.

(14) Zhang, J.; Schmalz, H.-G. *Angew. Chem., Int. Ed.* **2006**, *45*, 6704.

**Scheme 2**

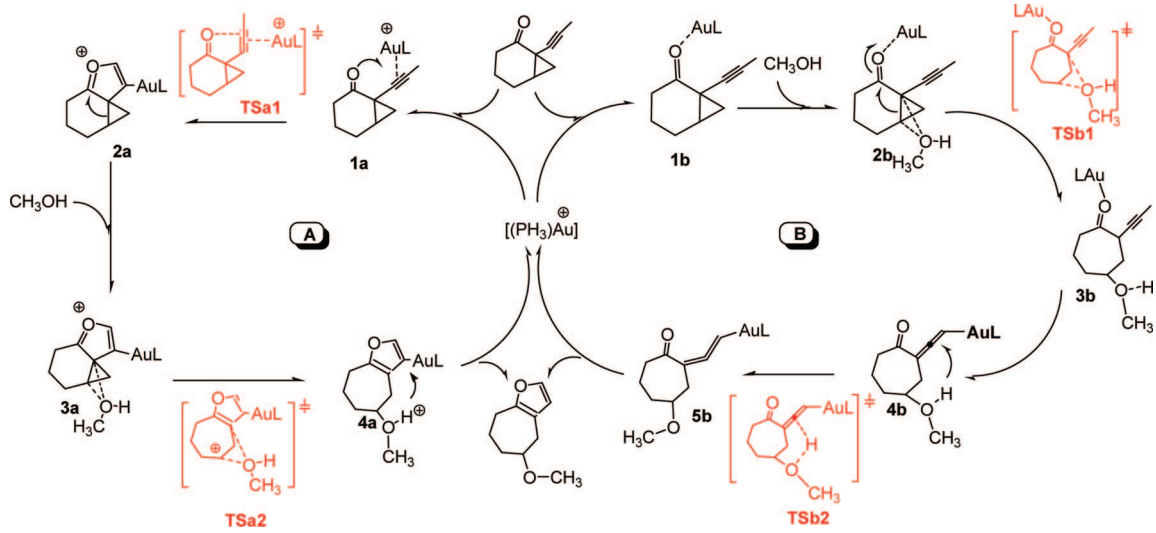


about the factors that control the activation barriers of this important reaction and also further investigate the effects of solvent on the thermodynamic and kinetic properties of these reactions.

## 2. Computational Methods

Geometries, energies, and first- and second-energy derivatives of all of the stationary points found here were fully optimized by hybrid density functional theory (DFT) using the GAUSSIAN 03 program suite.[15] Exchange and correlation were treated by the BHandHLYP method, which is based on Becke's half-and-half method[16] and the gradient-corrected correlation functional of Lee and co-workers.[17] This hybrid DFT method has been shown to be quite reliable for finding both the geometries and energies.[18] The 6-31G[19] basis set with polarization (d) and (p) were selected for all the atoms except gold, for which the Stuttgart−Dresden effective core potential[20] was utilized to accurately account for relativistic effects and to substantially reduce the number of electrons in the system. Vibrational frequency calculations done at the BH and HLYP /6-31G(d, p) level of theory were used to characterize all of the stationary points as either minima (the number of imaginary frequencies (NIMAG=0) or transition states (NIMAG=1)). The relative energies are, thus, corrected for the vibrational zero-point energies (ZPE, not scaled). In several significant cases, intrinsic reaction coordinate (IRC)[21] calculations were performed to unambiguously connect the transition states with the reactants and the products. To consider the effect of the solvent on the reactions of interest, the polarized continuum model (PCM) was applied,[22−24] and single-point energy calculations were done at the BH and HLYP/PCM/6-311++G(d, p)// BH and HLYP/6-31G(d, p) (SDD for Au) level of theory using the geometries along the minimum energy pathway. The dielectric constant was assumed to be 8.93 for bulk dichloromethane solvent.

## 3. Results and Discussions

Energy profiles for reaction pathways **a** and **b** are shown in Figures 1 and 2. The optimized geometries for the reactants (R1: $AuPH_3^+$; R2: 1-(1-alkynyl)cyclopropyl ketone; R3: $CH_3OH$ (the nucleophile of the reaction)), intermediates, transition states, and products of the reactions are depicted schematically in Figures 3 and 4 along with selected key geometry parameters (e.g., bond lengths). Their relative energies in the gas and solution phases, together with the activation barriers corresponding to the relevant transition structures, are shown in Table 1. Unless otherwise noted, the relative energies discussed in subsequent sections refer to the value in $CH_2Cl_2$ solvent. The detailed structural parameters and energies for the structures determined here are collected in the Supporting Information. In order to keep the computational cost low, the simplest model for the original cyclopropyl ketone was selected with gold's ligand $PPh_3$ replaced with $PH_3$. We note that the reaction still takes place experimentally for the simplest model compound where gold's ligand $PPh_3$ is replaced with $PH_3$ but has a lower yield[14] than the original cyclopropyl ketone reaction.

**3.1. Pathway a: Gold Functions Simply As a Transition Metal (coordination reaction between the terminal CC triple bond and the gold atom).** The energy profile for this process is represented in Figure 1. The structures of the various critical points located on the potential surface along with the values of the most relevant geometry parameters are shown in Figure 3. From the energy profile, it is evident that the first step of pathway **a** involves a preliminary intermediate **1a**, where the terminal CC triple bond interacts with the gold atom. If we consider $AuPH_3$ (I) as the "active" species of the catalyst, **1a**

(15) Frisch, M. J.; et al. *GAUSSIAN 03* (Revision D01); Gaussian, Inc.: Pittsburgh, PA, 2004.
(16) Becke, A. D. *J. Chem. Phys.* **1993**, *98*, 1372.
(17) Lee, C.; Yang, W.; Parr, R. G. *Phys. Rev. B* **1988**, *37*, 785.
(18) (a) Truong, T. N.; Duncan, W. *J. Chem. Phys.* **1994**, *101*, 7403. (b) Zhang, Q.; Bell, R.; Truong, T. N. *J. Phys. Chem.* **1995**, *99*, 592. (c) Durant, J. L. *Chem. Phys. Lett.* **1996**, *256*, 595. (d) Lynch, B. J.; Fast, P. L.; Harris, M.; Truhlar, D. G. *J. Phys. Chem. A* **2000**, *104*, 4811. (e) Espinosa-García, J. *J. Am. Chem. Soc.* **2004**, *126*, 920. (f) U. Wille, U.; Tan, J. C.-S.; Mucke, E.-K. *J. Org. Chem.* **2008**, *73*, 5821.
(19) (a) Rassolov, V. A.; Ratner, M. A.; Pople, J. A.; Redfern, P. C.; Curtiss, L. A. *J. Comput. Chem.* **2001**, *22*, 976. (b) Rassolov, V. A.; Pople, J. A.; Ratner, M. A.; Windus, T. L. *J. Chem. Phys.* **1998**, *109*, 1223.
(20) Andrae, D.; Häussermann, U.; Dolg, M.; Stoll, H.; Preuss, H. *Theor. Chim. Acta* **1990**, *77*, 123.
(21) Gonzalez, C.; Schlegel, H. B. *J. Chem. Phys.* **1989**, *90*, 2154.
(22) Tomasi, J.; Persico, M. *Chem. Rev.* **1994**, *94*, 2027.
(23) Mineva, T.; Russo, N.; Sicilia, E. *J. Comput. Chem.* **1998**, *19*, 290.
(24) Cossi, M.; Scalmani, G.; Rega, N.; Barone, V. *J. Chem. Phys.* **2002**, *117*, 43.

(25) Such type of transition metal-catalyzed oxonium ion formation is known in the case of the compound containing alkynes tethered with carbonyl groups; see: (a) Asao, N.; Aikawa, H.; Yamamoto, Y. *J. Am. Chem. Soc.* **2004**, *126*, 7458. (b) Asao, N.; Nogami, T.; Lee, S.; Yamamoto, Y. *J. Am. Chem. Soc.* **2003**, *125*, 10921. (c) Kusama, H.; Funami, H.; Shido, M.; Hara, Y.; Takaya, J.; Iwasawa, N. *J. Am. Chem. Soc.* **2005**, *127*, 2709. (d) Zhu, J.; Germain, A. R.; Porco, J. A., Jr. *Angew. Chem., Int. Ed.* **2004**, *43*, 1239.

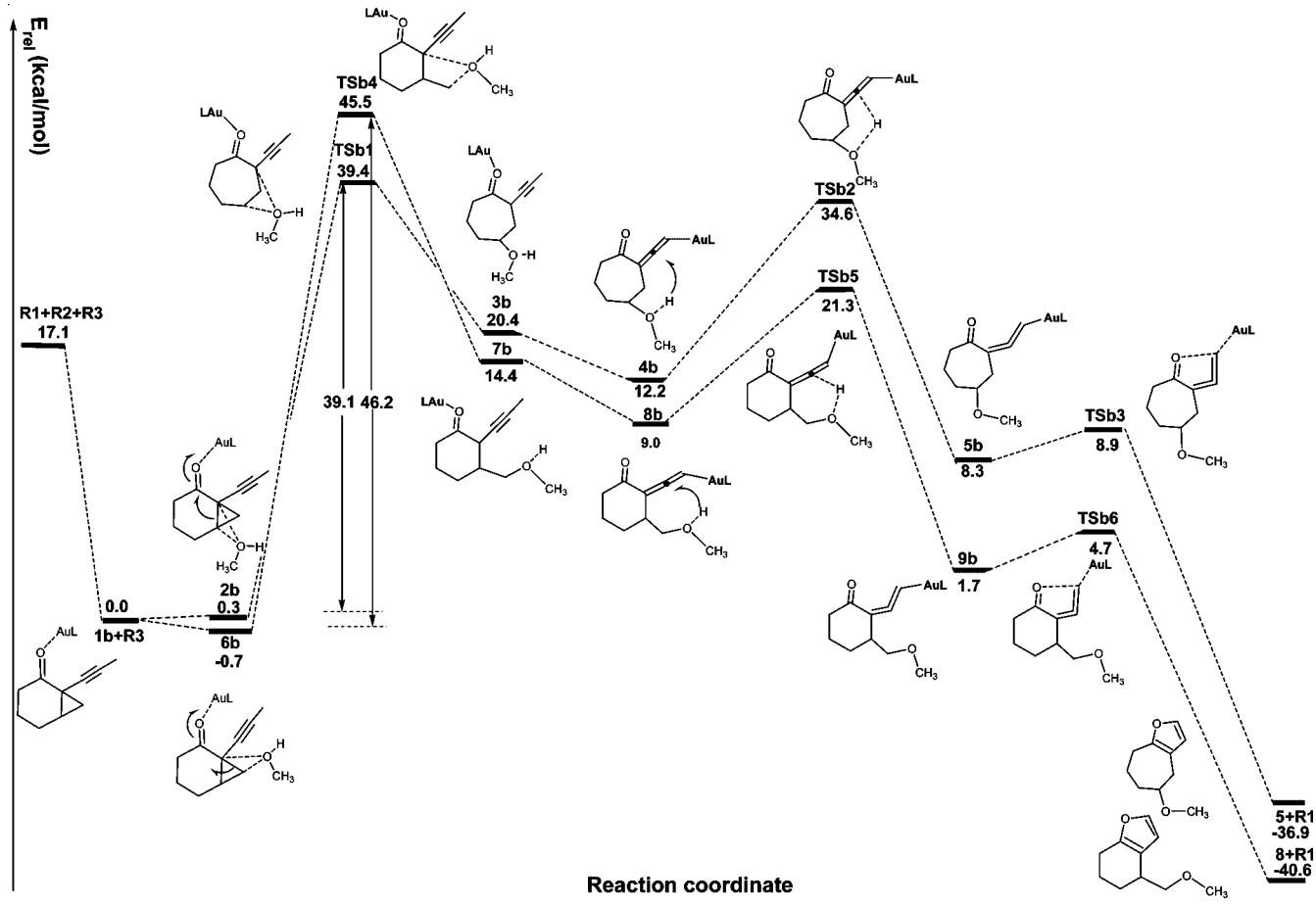


**Figure 2.** Energy profiles for path **b**; the relative energies are given in kcal/mol.

forms without any barrier and is 16.2 kcal/mol lower in energy than the reactants [$AuPH_3$ (I) (R1) + cyclopropyl ketone (R2)]. In **1a**, the lengths of the two Au−C bonds are 2.401 and 2.315 Å and the distance of Au−$O^6$ is 2.584 Å. The $C^4$−$C^5$ bond has lost a little of its triple-bond character and is now 1.217 Å (1.201 Å in R2). Meanwhile, the $O^6$−$C^7$ bond has undergone little change from 1.195 Å (in R2) to 1.213 Å. Once in **1a**, the coordination of the triple bond with the gold atom enhances the electrophilicity of the triple bond that induces a cyclization of the carbonyl oxygen onto the triple bond. A new and stable resonance structure intermediate **2a** is formed through **TSa1** (**TSa1** has only one imaginary frequency of 224i $cm^{-1}$, and IRC calculations confirmed that this TS connects the corresponding reactants and intermediate). Inspection of Figure 1 shows that the gold atom is completely connected with the $C^4$ atom of the alkyne (the bond distance Au−$C^4$ is 2.147 Å) in **TSa1**. Furthermore, the bonds of the $C^4$−$C^5$ and $C^5$−$O^6$ atoms change from 1.217 to 1.240 and 3.649 to 2.431 Å. The transition vector obtained from the frequency computations on **TSa1** is dominated by the $C^5$−$O^6$ and $C^4$−$C^5$ distances. Inspection of Table 1 shows that the energy of activation for this step is calculated to be 10.8 kcal/mol for **TSa1** and the energy of reaction for the **2a** intermediates is −10.6 kcal/mol with respect to **1a**. In **2a**, it is evident that the $C^4$−$C^5$ triple bond completes its change from a triple bond to a double bond (1.334 Å) and the $C^5$−$O^6$ bond becomes completely formed (1.414 Å). The $C^7$−$O^6$ bond also has some double-bond character and is now 1.283 Å. Furthermore, the NBO charges for the $C^2$, $C^3$, and $C^4$ atoms are 0.176, 0.119, and 0.034 eu, respectively. The structure and NBO charges both indicate that **2a** has oxonium ion character and also appears to have some carbocation character. The carbocation **2** intermediate proposed by Zhang and Schmalz[14] in Scheme 1 appears not to be a minimum energy structure on the potential energy surface, and our calculations provided a resonance structure intermediate **2a** in place of carbocation **2** as the intermediate structure.[24] The computational results suggest that it is unsuitable to use $Et_3SiH$ as a potential hydride source in place of a nucleophile to hypothesize the mechanism.[14] Our calculation results here are in good agreement with the experimental observation that no reaction was observed when $Et_3SiH$ was used as a potential hydride source in place of a nucleophile.

In principle, the strained carbon−carbon single bonds $C^1$−$C^2$ and $C^1$−$C^3$ can be further activated due to the presence of the carbonyl group. Inspection of Figure 1 shows that the attack of the oxygen atom of $CH_3OH$ on the $\sigma$ bond of $C^1$−$C^2$ or $C^1$−$C^3$ of the **2a** leads to the two different "ylide-like complexe" precursor complexes **3a** and **6a**, which have long C−O bonds. For instance, the distances of $C^1$−$O^8$ and $C^2$−$O^8$ for **3a** are 4.015 and 3.288 Å, and the distances of $C^1$−$O^8$ and $C^3$−$O^8$ for **6a** are 3.625 and 4.461 Å. Such large bond lengths are also reflected in the calculated complexation energies. For instance, our DFT results predict the binding energies relative to those of their corresponding reactants are −0.4 and −1.4 kcal/mol, respectively. The interaction of the lone pair electrons on the oxygen atom of methanol with the C−C $\sigma$ bond orbital on the cyclopropane moiety will yield new organogold intermediates (**4a** and **7a**) through formation of a C−O bond and cleavage of a C−C bond through transition states **TSa2** and **TSa4** (**TSa2** and **TSa4** have only one imaginary frequency of 239i and 330i $cm^{-1}$, respectively, and IRC calculations confirmed that these TSs connect the corresponding reactants and intermediates). In

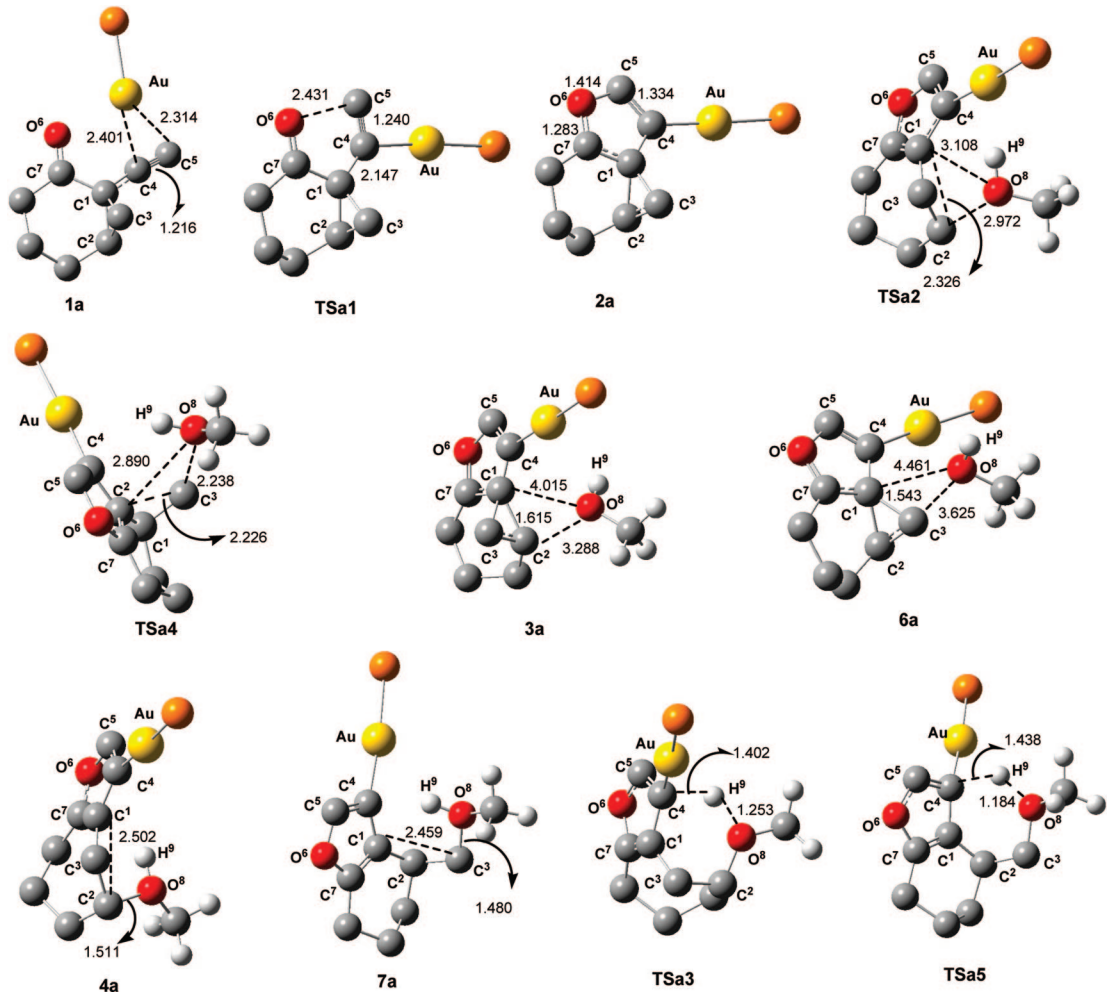


**Figure 3.** Optimized structures for path **a** shown in Figure 1, with selected structural parameters (bond lengths in Å).

**TSa2** and **TSa4**, the distances of $C^2-O^8$ and $C^3-O^8$ are shortened from 3.288 (**3a**) to 2.353 Å and 3.625 (**6a**) to 2.238 Å, respectively. Furthermore, the $C^1-C^2$ and $C^1-C^3$ bonds are stretched from 1.615 to 2.326 Å and 1.543 to 2.226 Å, respectively. As the reaction goes from **TSa2** and **TSa4** to **4a** and **7a**, the $C^2-O^8$ (1.511 Å) and $C^3-O^8$ (1.480 Å) bonds are completely formed and the $C^1-C^2$ (2.502 Å) and $C^1-C^3$ (2.459 Å) bonds become completely broken. The NBO charges for the $C^2$ and $C^3$ atoms were 0.325, −0.548 and −0.348, 0.095 eu for **TSa2** and **TSa4**, respectively. A positive charge found for the $C^2$ and $C^3$ atoms indicates that conversion from the resonance structures of the oxonium ion and carbocation to the carbocation intermediate has been accomplished in this step. It is important to point out that this step also is the rate-determining one. It is interesting to note that the carbocation **2** intermediate proposed by Zhang and Schmalz in Scheme 1 was found and characterized as a transition structure on the potential energy surface by our calculations. The cleavage of the C−C bond is strongly favored kinetically in the case of the $C^1-C^2$ bond and required only 19.8 kcal/mol of energy, while the activation energy for the cleavage of the $C^1-C^3$ bond is 31.8 kcal/mol. The higher activation barriers for **TSa4** indicate that the ring-opening cycloisomerization for cyclopropyl ketones has a high regioselectivity. The lower barriers found for **TSa2** can mainly be attributed to the following reasons. First, the DFT calculations show that forming the C−O bond in the **TSa2** and **TSa4** structures is shortened by 54% and 59%, respectively, with respect to the corresponding intermediates (see Figure 1). These structural features reveal that the former transition structures take on more reactant-like character than later ones. According to the Hammond postulate,[26] the former should have lower activation barriers, and the latter, higher activation barriers. Second, the $C^1-C^2$ bond is not only affected by the ring strain of the cyclopropyl moiety but also affected by the ring strain of the six-membered ring, which makes the cleavage of the $C^1-C^2$ bond more feasible than that of the $C^1-C^3$ bond. Finally, the value of the NBO charges for the $C^2$ (0.325 eu for **TSa2**) and $C^3$ (0.095 eu for **TSa4**) atoms indicate that the attack of the $C^1-C^2$ bond is more feasible than that of the $C^1-C^3$ bond by $CH_3OH$ (a nucleophile). Thus, less energy is needed for **TSa2** to go from the intermediates to the transition states than for **TSa4**.

The subsequent step for migration of the hydrogen atom results in the formation of the final product (**5** and **8**) and regeneration of the catalyst (R2). The final barriers of 14.9 and 5.1 kcal/mol are required to release the product and regenerate the catalyst (transition states **TSa3** and **TSa5**). These final steps are exothermic by −27.7 and −29.6 kcal/mol, respectively, and the whole catalytic processes are exothermic by −37.9 and −41.5 kcal/mol lower than reactants. It is worth noting that these computations agree very well with the experimental results obtained by Zhang and Schmalz.[14]

**3.2. Pathway b: Gold Functions As Both a Lewis Acid and a Transition Metal (coordination reaction between the carbonyl oxygen and the gold atom).** Cationic Au(I) species are better Lewis acids compared with other group 11

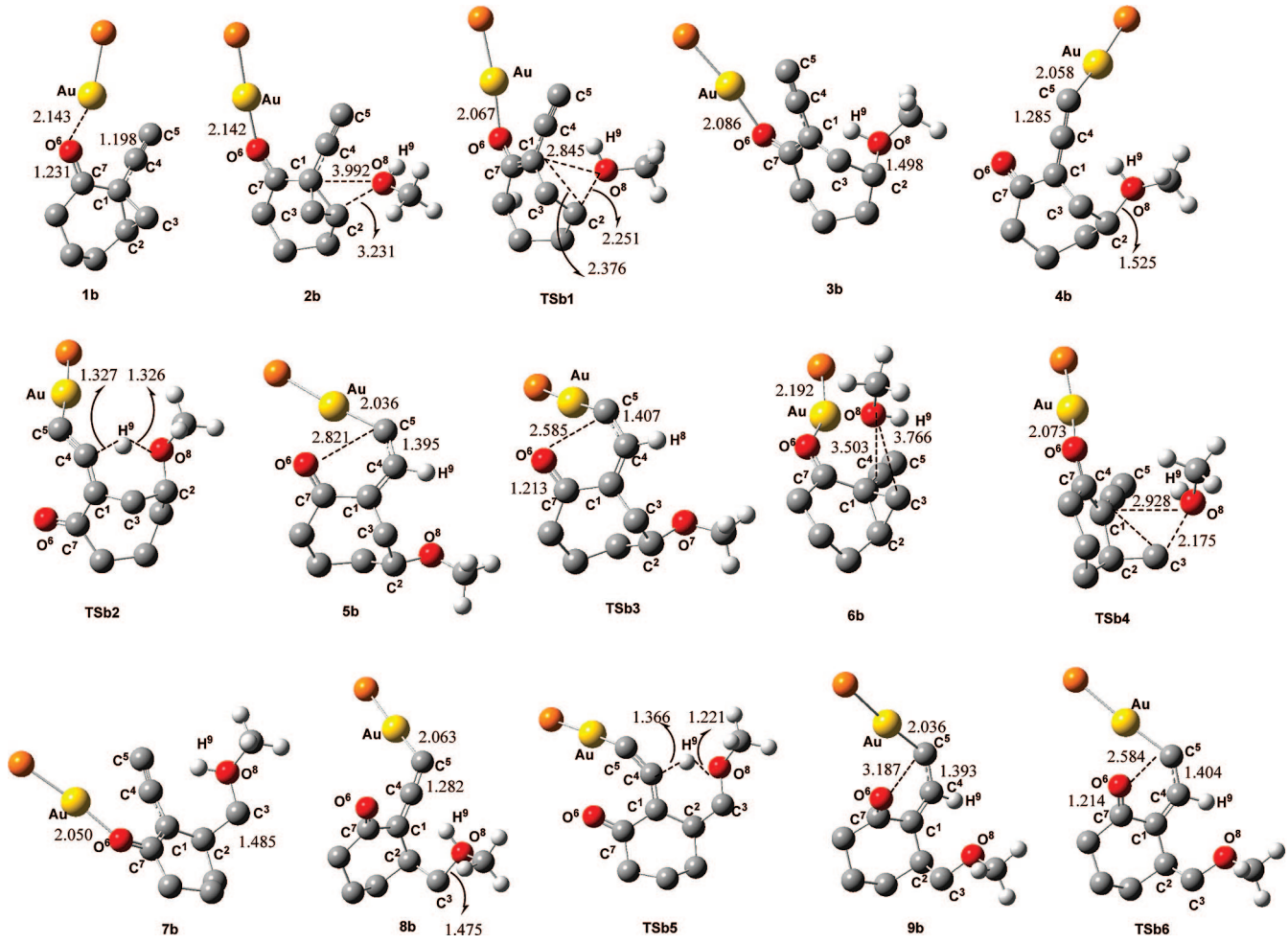


**Figure 4.** Optimized structures for path **a** shown in Figure 2, with selected structural parameters (bond lengths in Å).

metals for many transformations. It appears that relativistic contraction of the valence s or p orbitals of Au should be responsible for this since they should correspond to a relatively low-lying lowest unoccupied molecular orbital (LUMO) and therefore have strong Lewis acidity. This conclusion can also be obtained from consideration of the high electronegativity of Au (2.4, compared with 1.9 for Ag): strong Lewis acidity generally correlates with electronegativity (provided that a coordination site is available for accepting an electron pair). Thus, gold can function as both a Lewis acid and a transition metal and give rise to another possible reaction pathway. The energy profile for this process is depicted in Figure 2. The structures of the various critical points located on the potential surface along with the values of the most relevant geometry parameters are presented in Figure 4. Examination of Figure 2 shows that the first step for pathway **b** also involves a preliminary intermediate **1b** stabilized by the coordination of the Au atom to the carbonyl oxygen atom and the $\pi$ bond of the alkyne moiety. If we consider $AuPH_3$ (I) as the "active" form of the catalyst, **1a** forms without any barrier and is 17.1 kcal/mol lower than the reactants [$AuPH_3$ (I) (R1) + cyclopropyl ketone (R2)]. In **1b**, the distance of Au−$O^6$ is 2.144 Å and the lengths of the two Au−C bonds are 3.033 and 3.120 Å. The $O^6$−$C^7$ bond undergoes little change from 1.195 Å (in R3) to 1.231 Å. Comparison of the structures of 1**b** with 1**a** reveals that the major coordination reaction occurs between the carbonyl oxygen atom and the gold atom in **1b**. However, the major coordination reaction takes place between the terminal CC triple bond and the gold atom in **1a**. Once in **1b**, the coordination of the carbonyl oxygen atom with gold atom facilitates the homo-Michael-type addition of the $CH_3OH$ molecule to the carbon−carbon $\sigma$ bond of the cyclopropyl moiety. Examination of Figure 2 suggests that the attack of the oxygen atom of the $CH_3OH$ molecule on the $\sigma$ bond of the $C^1$−$C^2$ or $C^1$−$C^3$ bonds of **1b** first leads to the two different "ylide-like complexes", **2b** and **6b**, that have a long C−O bond. Inspection of Figure 4 shows that the distances of $C^1$−$O^8$ and $C^2$−$O^8$ for **2b** are 3.992 and 3.231 Å and the distances of $C^1$−$O^8$ and $C^3$−$O^8$ for **6b** are 3.504 and 3.767 Å, respectively. Such large bond lengths are also reflected in the calculated complexation energies. For instance, our DFT results predict the binding energies relative to those of their corresponding reactants are 0.4 (−4.9 kcal/mol in the gas phase) and −1.4 (−7.6 kcal/mol in the gas phase) kcal/mol, respectively. The homo-Michael-type addition of the $CH_3OH$ to the carbon−carbon $\sigma$ bond of the cyclopropyl moiety will yield intermediates **3b** and **7b** through **TSb1** and **TSb4** (**TSb1** and **TSb4** have only one imaginary frequency of 294i and 366i $cm^{-1}$, respectively, and IRC calculations confirmed that these TSs connect the corresponding reactants and intermediates). Similar to pathway **a**, this step is also the rate-determining one. Compared with **2b** and **6b**, the distances of $C^2$−$O^8$ and $C^3$−$O^8$ for **TSb1** and **TSb4** are 2.252 and 2.175 Å, respectively. Furthermore, the bonds of $C^1$−$C^2$ and $C^1$−$C^3$ are elongated by 0.831 and 0.744 Å, respectively. As the reaction goes from **TSb1** and **TSb4** to **3b** and **7b**, the $C^2$−$O^8$ and $C^3$−$O^8$ bonds for **3b** and **7b** are 1.498 and 1.485 Å, respectively, and

(26) Hammond, G. S. *J. Am. Chem. Soc.* **1955**, *77*, 334.

**Table 1. Thermodynamic Properties (relative energies and activation energies in gas phase and in solution) of the Structures in Figures 1 and 2[a]**

| species | $\Delta E^{rel}{}_{gas}$ | $\Delta E^{\Delta}{}_{gas}$ | $\Delta E^{rel}{}_{sol}$ | $\Delta E^{\Delta}{}_{sol}$ |
|---|---|---|---|---|
| **1a** + R3 | 0.0 | | 0.0 | |
| **TSa1** + R3 | 14.6 | 14.6 | 10.8 | 10.8 |
| **2a** + R3 | −12.6 | | −10.6 | |
| **3a** | −19.7 | | −11.0 | |
| **TSa2** | 2.5 | 22.2 | 8.8 | 19.8 |
| **4a** | −14.8 | | −10.2 | |
| **TSa3** | −7.7 | 7.18 | 4.7 | 14.9 |
| **5** + R1 | −44.1 | | −37.9 | |
| **6a** | −19.7 | | −12.0 | |
| **TSa4** | 12.1 | 31.8 | 19.8 | 31.8 |
| **7a** | −18.1 | | −11.9 | |
| **TSa5** | −18.6 | −0.5 | −6.8 | 5.1 |
| **8** + R1 | −48.3 | | −41.5 | |
| **1b** | 0.0 | | 0.0 | |
| **2b** | −4.9 | | 0.3 | |
| **TSb1** | 34.4 | 39.3 | 39.4 | 39.1 |
| **3b** | 13.9 | | 20.4 | |
| **4b** | 12.3 | | 12.2 | |
| **TSb2** | 24.9 | 12.6 | 34.6 | 22.4 |
| **5b** | −0.3 | | 8.3 | |
| **TSb3** | 0.9 | 1.2 | 8.9 | 0.6 |
| **5** + R1 | −44.4 | | −36.9 | |
| **6b** | −7.6 | | −0.6 | |
| **TSb4** | 39.2 | 46.8 | 45.5 | 46.1 |
| **7b** | 10.5 | | 14.4 | |
| **8b** | 7.2 | | 9.0 | |
| **TSb5** | 10.6 | 3.4 | 21.3 | 12.3 |
| **9b** | −6.3 | | 1.7 | |
| **TSb6** | −4.4 | 1.9 | 4.7 | 3.0 |
| **8** + R1 | −48.6 | | −40.6 | |

[a] These values, in kcal/mol, were calculated at the BH and HLYP/6-31G** (SDD for Au) level of theory and included the zero-point energy correction, using single-point PCM calculations at the BH and HLYP/PCM/6-311++G(d, p)//BH and HLYP/6-31G(d, p) (SDD for Au) level of theory to model the effect of the solvent ($CH_2Cl_2$).

the $C^1-C^2$ and $C^1-C^3$ bonds are 2.502 and 2.459 Å, respectively. These changes in the bond distances show that the $C^2-O^8$ and $C^3-O^8$ bonds are completely formed and the $C^1-C^2$ and $C^1-C^3$ bonds become completely broken. Inspection of Table 1 shows that this endothermic homo-Michael-type addition step (by 20.1 and 15.1 kcal/mol, respectively) proceeds with a very high activation energy (39.1 and 46.1 kcal/mol, respectively). We have already demonstrated that this step is the rate-determining one, and thus the higher activation barriers for **TSb1** and **TSb4** than **TSa2** and **TSa4** indicate that pathway **b** is an unfavorable pathway. The higher barriers found for **TSb1** and **TSb4** compared to those for **TSa2** and **TSa4** can mainly be attributed to the following reasons. Comparison of the **TSb1** and **TSb4** and **TSa2** and **TSa4** structures shows that due to the presence of the resonance structures, the strained carbon−carbon single bonds $C^1-C^2$ and $C^1-C^3$ can be easily activated in the **TSa2** and **TSa4** structures. The higher activation barriers for **TSb4** indicate that the ring-opening cycloisomerization for cyclopropyl ketones also has a high regioselectivity for pathway **b**. The lower barriers found for **TSb1** can also mainly be attributed to the following reasons. First, the DFT calculations show that forming the C−O bond in the **TSb1** and **TSb4** structures shortens this bond distance by 30% and 42%, respectively, than in the corresponding intermediates. These structural features reveal that the former transition structures take on more reactant-like character than product-like character, and the Hammond postulate[26] predicts the former should have lower activation barriers. Second, the $C^1-C^2$ bond is affected by the ring strain of both the cyclopropyl moiety and the six-membered ring, which makes the cleavage of the $C^1-C^2$ bond more feasible than the $C^1-C^3$ bond. Finally, the values of the NBO charges for the $C^2$ (0.300 eu for **TSb1**) and $C^3$ (0.065 eu for **TSb4**) atoms indicate that attack of the $C^1-C^2$ bond is more feasible than that of the $C^1-C^3$ bond by $CH_3OH$. Thus, a lower energy is needed for **TSb1** to go from the intermediates to the transition states than for **TSb4**.

To accomplish a cyclization of the carbonyl oxygen onto the triple bond, there is subsequent coordination of the alkynyl moiety of the alkenynone **3b** and **7b** to $AuCl_3$, resulting in the formation of new intermediates **4b** and **8b**, where the terminal CC triple bond interacts with the gold atom. **4b** and **8b** are 8.2 and 5.4 kcal/mol lower in energy than **3b** and **7b**, respectively, but remain 11.9 and 9.7 kcal/mol higher than the reactants. This indicates that the CC triple bond interaction with the gold atom is significantly stronger than that between the gold atom and the carbonyl oxygen atom. In **4b** and **8b**, the bond distance $Au-C^5$ is 2.058 and 2.043 Å, respectively. Furthermore, the $C^4-C^5$ bond has almost lost its triple-bond character and now has bond lengths of 1.285 and 1.282 Å, respectively. The subsequent step for migration of the hydrogen atom results in the formation of new vinyl-Au intermediates **5b** and **9b**, which are 8.0 and 2.4 kcal/mol higher in energy than the reactants. Similar intermediates have also been observed to be trapped by other electrophiles in an intramolecular fashion.[27−29] The vinyl-Au intermediates **5b** and **9b** will proceed to the final product (**5** and **8**) and regenerate the catalyst (R2) via cyclization transition states **TSb3** and **TSb6** (see Figure 2), which have barriers of 14.9 and 5.1 kcal/mol and are exothermic by 45.2 and 42.3 kcal/mol, respectively. The entire catalytic processes are exothermic by −37.9 and −41.5 kcal/mol lower than the starting reactants.

## 4. Conclusion

In summary, this work has provided the first theoretical study for the reaction of gold(I)-catalyzed synthesis of highly substituted furans based on 1-(1-alkynyl)cyclopropyl ketones with nucleophiles. Our calculations suggest that the first step of the catalytic cycle is the cyclization of the carbonyl oxygen onto the triple bond to form a new and stable resonance structure of an oxonium ion and a carbocation intermediate. The attack of the carbonyl oxygen to the gold-coordinated alkynes resulted in the formation of the resonance structure of an oxonium ion and carbocation intermediate **2a**, which upon subsequent trapping with alcohols was followed by migration of the hydrogen atom to form the final product (**5** and **8**) and regeneration of the catalyst (R2). The key reaction step in the catalytic cycle is the attack of the oxygen atom of the $CH_3OH$ nucleophile on the C−C $\sigma$ bond of the cyclopropane moiety to yield new organogold intermediates through formation of a C−O bond and cleavage of a C−C bond via a transition state. The cleavage of the C−C bond is strongly favored kinetically in the case of the $C^1-C^2$ bond and needs only 19.8 kcal/mol of energy. The higher activation energy of 31.8 kcal/mol needed for cleavage of the $C^1-C^3$ bond indicates that the ring-opening cycloisomerization for cyclopropyl ketones has a high regioselectivity. Our computational results are consistent with the experimental observations of Zhang and Schmalz for gold(I)-catalyzed transformations to highly substituted furans.[14]

**Acknowledgment.** We gratefully acknowledge the National Natural Science Foundation of China (Grant No.

(27) Zhang, L. M. *J. Am. Chem. Soc.* **2005**, *127*, 16804.
(28) Nakamura, I.; Sato, T.; Yamamoto, Y. *Angew. Chem., Int. Ed.* **2006**, *45*, 4473.

20673149), the Natural Science Foundation of Guangdong Province (Grant No. 7003709) to C.Y.Z., and the Hong Kong Research Grants Council (HKU/7040/06P) to D.L.P. for the financial support of this research. We are grateful to the reviewers for their invaluable suggestions and Prof. Zhenyang Lin for his helpful discussions.

**Supporting Information Available:** The complete citation for ref 14, the Cartesian coordinates for the calculated stationary structures, and the sum of the electronic and zero-point energies for the transition and ground states obtained from the DFT calculations are given. This material is available free of charge via the Internet at http://pubs.acs.org.

OM800751U

(29) Dube, P.; Toste, F. D. *J. Am. Chem. Soc.* **2006**, *128*, 12062.